Heliyon 10 (2024) e34562

Contents lists available at ScienceDirect

Heliyon

journal homepage: www.cell.com/heliyon

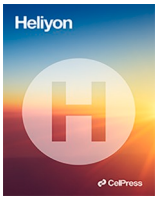

Research article

Subchronic particulate matter exposure underlying polyhexamethylene guanidine phosphate–induced lung injury: Quantitative and qualitative evaluation with chest computed tomography

Cherry Kim [a,1], Sang Hoon Jeong [b,1], Hong Lee [b], Yoon Jeong Nam [b], Hyejin Lee [b], Jin Young Choi [b], Yu-Seon Lee [b], Jaeyoung Kim [b], Yoon Hee Park [b], Ju-Han Lee [c,*]

[a] *Department of Radiology, Ansan Hospital, Korea University College of Medicine, 123, Jeokgeum-ro, Danwon-gu, Ansan-si, Gyeonggi, 15355, South Korea*

[b] *Medical Science Research Center, Ansan Hospital, Korea University College of Medicine, 123, Jeokgeum-ro, Danwon-gu, Ansan-si, Gyeonggi, 15355, South Korea*

[c] *Department of Pathology, Ansan Hospital, Korea University College of Medicine, 123, Jeokgeum-ro, Danwon-gu, Ansan-si, Gyeonggi, 15355, South Korea*

A B S T R A C T

Our study was to explore the effects of subchronic particulate matter (PM) exposure on lung injury induced by polyhexamethylene guanidine phosphate (PHMG-p) in a rat model. Specifically, we investigated pulmonary inflammation, fibrosis, and tumor formation using chest computed tomography (CT), and histopathologic examination. PHMG-p was administered intratracheally to 20 male rats. After an initial week of PHMG-p treatment, the experimental group (PM group) received intratracheal administration of PM suspension, while the control group received normal saline. This regimen was continued for 10 weeks to induce subchronic PM exposure. Chest CT scans were conducted on all rats, followed by the extraction of both lungs for histopathological analysis. All CT images underwent comprehensive quantitative and qualitative analyses. Pulmonary inflammation was markedly intensified in rats subjected to subchronic PM exposure in the PM group compared to those in the control. Similarly, lung fibrosis was more severe in the PM group as observed on both chest CT and histopathologic examination. Quantitative chest CT analysis revealed that the mean lesion volume was significantly greater in the PM group than in the control group. Although the incidence of bronchiolo-alveolar hyperplasia was higher in the PM group compared to the control group, this difference was not statistically significant. In summary, subchronic PM exposure exacerbated pulmonary inflammation and fibrosis underlying lung injury induced by PHMG-p.

1. Introduction

Elevated levels of particulate matter (PM) in the air represent a major global health risk, contributing significantly to increased morbidity and mortality rates, as well as to the overall global disease burden [1,2]. Recent research has demonstrated a strong association between PM levels and the incidence of lung cancer across four national cohorts [3]. Furthermore, both short-term and long-term exposure to PM have been demonstrated to impair lung function in children, older adults, and even healthy young adults [4–6]. Additionally, PM exposure has also been linked to higher mortality rates in patients with pre-existing fibrotic interstitial lung

Abbreviations: PHMG-p, polyhexamethylene guanidine phosphate; PM, particulate matter; GGO, ground-glass opacity; HU, Hounsfield units.

* Corresponding author.
E-mail address: repath@korea.ac.kr (J.-H. Lee).

[1] Equally contributed.

https://doi.org/10.1016/j.heliyon.2024.e34562
Received 26 August 2023; Received in revised form 9 July 2024; Accepted 11 July 2024
Available online 14 July 2024

Table 1
Results of the qualitative CT analyses in the PM group and the control group.

	PM	Control	P-value
CT finding scores			
Consolidation	1.90 ± 1.29	0.30 ± 0.48	0.002
GGO	3.00 ± 0.94	1.00 ± 0.94	<0.001
Centrilobular nodules	2.60 ± 1.08	1.20 ± 1.40	0.022
Nodules	1.50 ± 1.08	0.70 ± 0.48	0.046
Masses	0.80 ± 0.92	0.20 ± 0.42	0.077
Bronchiectasis	3.00 ± 0.67	1.30 ± 0.68	<0.001
Linear opacities	2.90 ± 0.57	1.20 ± 0.79	<0.001
CT extent scores in each lobe			
Right, superior lobe	2.80 ± 1.14	1.50 ± 0.53	0.004
Right, middle lobe	2.20 ± 1.32	1.10 ± 0.88	0.041
Right, inferior lobe	3.10 ± 0.74	1.40 ± 0.97	<0.001
Postcaval lobe	3.20 ± 0.79	1.50 ± 1.18	0.001
Left, upper region	2.20 ± 0.63	1.00 ± 0.67	0.001
Left, middle region	2.10 ± 0.57	1.10 ± 0.74	0.003
Left, lower region	3.10 ± 0.74	1.60 ± 0.84	<0.001
Total CT scores	18.70 ± 3.43	9.20 ± 5.05	<0.001
CT inflammation score	4.90 ± 2.13	1.30 ± 0.82	<0.001
CT fibrosis score	5.90 ± 1.10	2.50 ± 1.43	<0.001

Note – CT, computed tomography; GGO, ground-glass opacity.

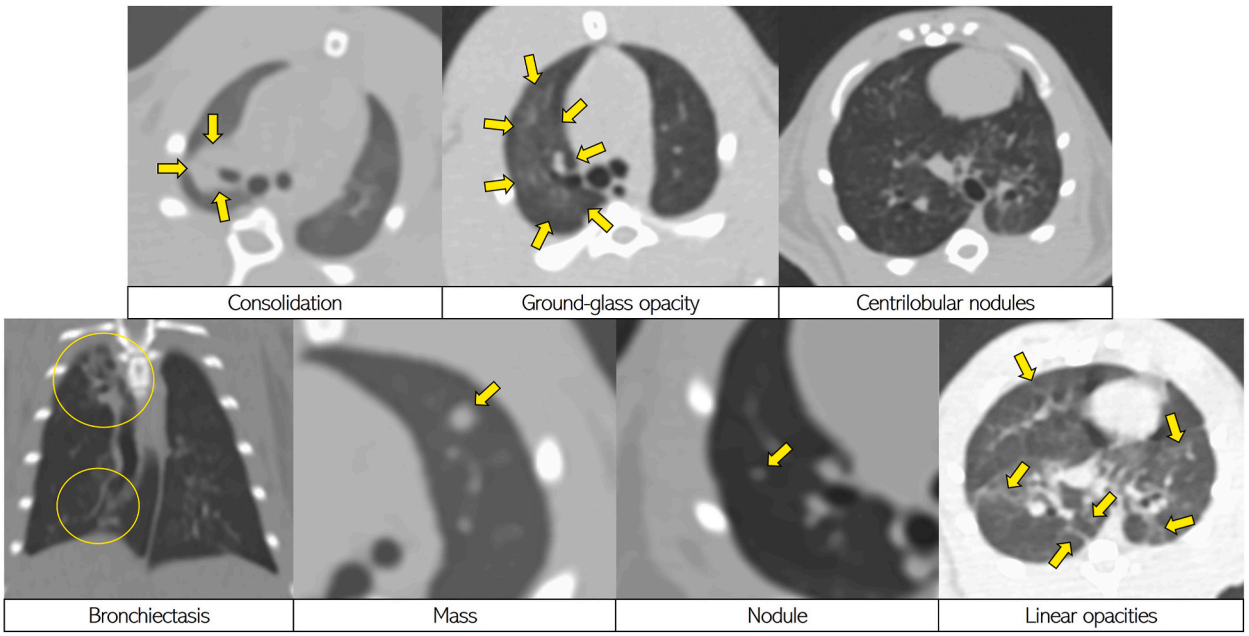

Fig. 1. Characteristic CT findings.

disease [7]. Our previous work indicated that subchronic exposure to PM exacerbates pulmonary fibrosis and inflammation in a bleomycin-induced lung fibrosis rat model [8].

Polyhexamethylene guanidine phosphate (PHMG-p) is well-known as an ingredient in humidifier disinfectants. Approximately 11 million individuals, accounting for 22 % of the general population in South Korea, have been exposed to substances contained in these disinfectants [9–11]. PHMG-p has been strongly linked to severe lung injuries, including lung fibrosis and tumors [12]. Over a 52-week observation period, the severity of pulmonary fibrosis and the occurrence of bronchiolo-alveolar hyperplasia markedly rose after intratracheal administration of PHMG-p in a rat model [13]. Therefore, exposure to both PHMG-p and air pollution due to PM could emerge as serious public health problems.

Chest computed tomography (CT) is the leading method for producing detailed cross-sectional images of the chest, allowing for accurate assessment of lung abnormalities [14]. In several rat studies, chest CT has been an effective tool for accurately evaluating lung lesions associated with exposure to PHMG-p [8,13,15]. In these studies, CT findings correlated with pathologic findings in long- and short-term PHMG-p–induced lung injury, such as pulmonary inflammation, fibrosis, and tumor formation, and chronological changes owing to PHMG-p exposure were well presented with chest CT and histopathologic analysis. Additionally, a previous study using a rat

Table 2
Comparison of quantitative analysis of CT results between the PM group and the control group.

	PM	Control	P-value
Lesion volume (mL)	2.96 ± 0.62	1.69 ± 0.57	<0.001
Lesion volume %	20.05 ± 3.69	11.83 ± 5.01	<0.001
Whole lung volume (mL)	14.79 ± 1.62	15.10 ± 3.60	0.793

Table 3
Histopathologic evaluation of inflammation and fibrosis in the PM group and the control group.

	PM	Control	P-value
Inflammation extent, n (%)			
None	0 (0 %)	0 (0 %)	0.025
Mild	3 (30 %)	8 (80 %)	
Moderate	7 (70 %)	2 (20 %)	
Severe	0 (0 %)	0 (0 %)	
Inflammation severity, n (%)			
None	0 (0 %)	0 (0 %)	0.043
Mild	0 (0 %)	2 (20 %)	
Moderate	6 (60 %)	8 (80 %)	
Severe	4 (40 %)	0 (0 %)	
Inflammation score	4.10 ± 0.74	3.00 ± 0.47	0.001
Fibrosis score	4.50 ± 0.53	3.80 ± 1.03	0.072

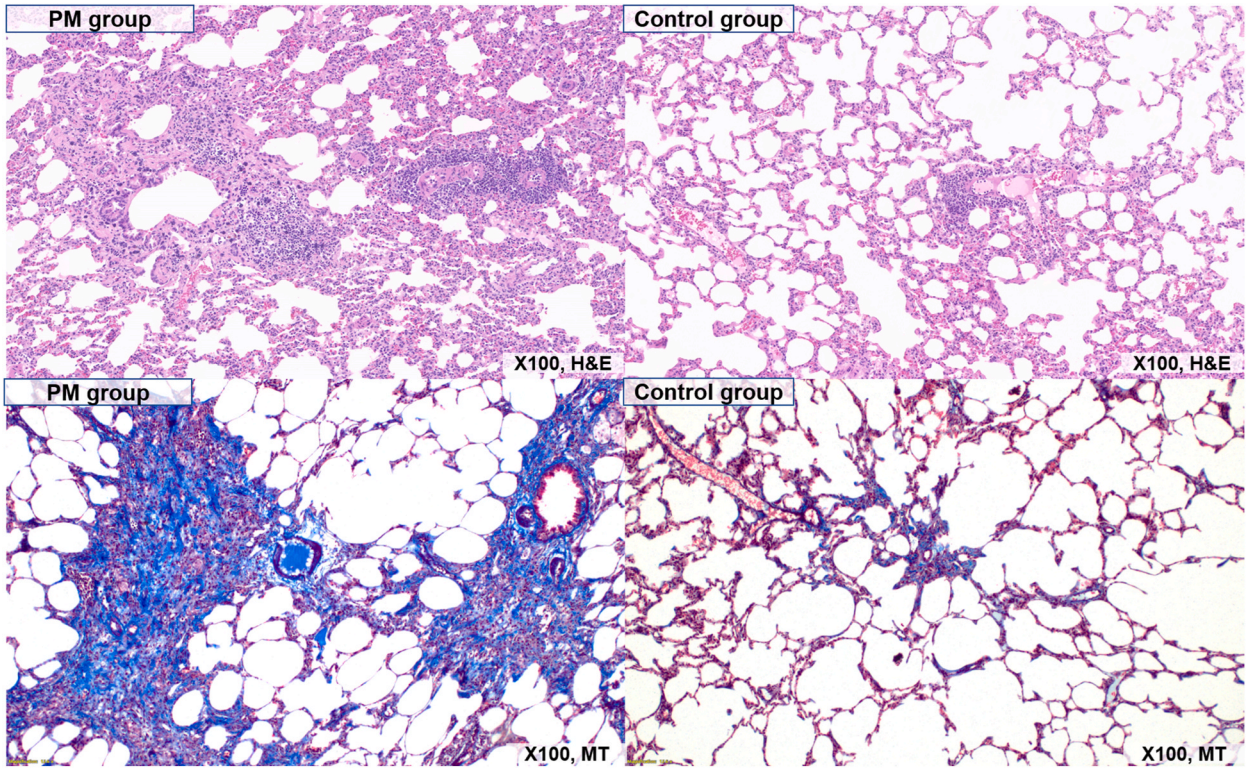

Fig. 2. Pathologic findings showing the differences in the extent and severity of inflammation and fibrosis between the PM group and the control. Inflammation and fibrosis are observed to be significantly more extensive in the PM group compared to the control group. (H&E, hematoxylin and eosin staining; MT, Masson's trichrome staining; X100).

model demonstrated that chest CT effectively demonstrated the effects of subchronic PM exposure underlying bleomycin-induced lung fibrosis [8]. However, that study evaluated CT findings with only qualitative analysis by a certified thoracic radiologist, and it is important to perform quantitative analyses of such lung lesions induced by bleomycin and subchronic exposure to PM in order to objectively evaluate them. Also, to our knowledge, there have been no reports on the effects of PM on PHMG-p-induced lung injury

Table 4
Comparison of bronchiolo-alveolar hyperplasia and bronchiolo-alveolar adenomas in the PM group and the control group.

	PM	Control	P-value
Mean number of bronchiolo-alveolar hyperplasia lesions	10.70 ± 6.55	8.70 ± 7.82	0.543
Number of rats with bronchiolo-alveolar hyperplasia	10 (100 %)	10 (100 %)	>0.999
Mean number of bronchiolo-alveolar adenomas	0.20 ± 0.42	0	0.151
Number of rats with bronchiolo-alveolar adenoma	2 (20 %)	0 (0 %)	0.136

using chest CT.

Therefore, our study was to explore the effects of subchronic PM exposure on lung injury induced by PHMG-p, including pulmonary inflammation, fibrosis, and tumor formation, in a rat model with both quantitative and qualitative evaluation of chest CT, as well as histopathologic evaluation.

2. Results

2.1. Qualitative CT analysis

The findings of the qualitative CT analysis are described in Table 1, with representative CT findings illustrated in Fig. 1. The mean CT finding scores showed significant differences between the PM group and the control group (all $P < 0.05$). The mean CT extent scores across all lobes were notably higher in the PM group compared to the control group (all $P < 0.05$). Additionally, the total CT scores were significantly elevated in the PM group compared to the control group (18.70 ± 3.43 vs. 9.20 ± 5.05, $P < 0.001$).

The PM group exhibited a significantly higher mean CT inflammation score (4.90 ± 2.13 vs. 1.30 ± 0.82, $P < 0.001$). Additionally, the average CT fibrosis score showed a significant increase in the PM group relative to the control group (5.90 ± 1.10 vs. 2.50 ± 1.43, $P < 0.001$).

2.2. Quantitative CT analysis

The comparison of the quantitative analyses of CT findings is shown in Table 2. The mean lesion volume of the PM group was significantly greater than that of the control group (2.96 ± 0.62 mL vs. 1.69 ± 0.57 mL, $P < 0.001$). The mean lesion volume percentage of the PM group was also significantly higher than that of the control group (20.05 % ± 3.69 % vs. 11.83 % ± 5.01 %, $P < 0.001$). The mean whole lung volume of the PM group was smaller than that of the control, although this difference was not statistically significant (14.79 ± 1.62 mL vs. 15.10 ± 3.60 mL, $P = 0.793$).

2.3. Histopathologic evaluations of inflammation and fibrosis

The result of histopathologic evaluation of inflammation and fibrosis in both groups are presented in Table 3 and Fig. 2. In the evaluations of the extent of inflammation, seven rats (70 %) exhibited moderate inflammation extent in the PM group, whereas two rats (20 %) in the control group exhibited moderate inflammation extent, with a significantly greater extent in the PM group ($P = 0.025$). In the inflammation severity analysis, four rats (40 %) exhibited severe inflammation, and six rats (60 %) exhibited moderate inflammation in the PM group; however, eight rats (80 %) exhibited moderate inflammation, and two rats (20 %) exhibited mild inflammation in the control, with significantly more severe inflammation in the PM group than in the control group ($P = 0.043$). The mean inflammation score was also significantly higher in the PM group than in the control group (4.10 ± 0.74 vs. 3.00 ± 0.47, $P = 0.001$).

The mean fibrosis score in the PM group was elevated compared to the control group, but the difference was not statistically significant (4.50 ± 0.53 vs. 3.80 ± 1.03, $P = 0.072$).

2.4. Bronchiolo-alveolar hyperplasia vs. bronchiolo-alveolar adenoma

Table 4 shows the comparison of bronchiolo-alveolar hyperplasia and bronchiolo-alveolar adenoma between the PM group and the control. All rats in both groups exhibited bronchiolo-alveolar hyperplasia (10 rats [100 %] in each group), with a slightly higher mean number of lesions observed in the PM group compared to the control group, although the difference was not statistically significant (10.70 ± 6.55 vs. 8.70 ± 7.82, $P = 0.543$).

Bronchiolo-alveolar adenoma was detected in two rats (20 %) in the PM group, but no bronchiolo-alveolar adenoma was detected in the control. The mean number of bronchiolo-alveolar adenoma lesions was higher in the PM group than in the control group (0.20 ± 0.42 vs. 0, $P = 0.151$), but this difference did not reach statistical significance.

3. Discussion

Our results revealed that subchronic PM exposure aggravated pulmonary inflammation, fibrosis, or tumor formation associated with PHMG-p exposure, as demonstrated by chest CT and histopathologic evaluation. Relative to the control group, pulmonary

inflammation was significantly aggravated in rats with subchronic PM exposure underlying PHMG-p–induced lung injury. Lung fibrosis was also worse in PM-exposed rats than in the control group on both chest CT and histopathologic evaluation, however, statistically significant differences were observed only in the CT fibrosis scores between the groups. In the quantitative chest CT analysis, the mean lesion volume was significantly higher in the PM group than in the control. The PM group showed a higher mean number of bronchiolo-alveolar hyperplasia lesions compared to the control, but this disparity did not reach statistical significance. Two bronchiolo-alveolar adenomas were detected only in the PM group.

Exposure to PM has been extensively studied and is known to have significant adverse health effects. PM, especially fine particles with diameters less than 2.5 μm ($PM_{2.5}$), can deeply penetrate the respiratory system and may even enter the bloodstream, leading to a range of health problems. The World Health Organization has recognized PM pollution as a significant global health risk, linking it to various cardiovascular and respiratory conditions, including asthma, bronchitis, chronic pulmonary disease, lung cancer, and stroke [16,17]. Additionally, in patients with underlying lung disease, such as lung fibrosis or asthma, the impact of PM exposure is important. There have been several reports of PHMG-induced lung injury [13,15,18,19], and one study demonstrated persistent lung fibrosis, including bronchiectasis and increased severity of pulmonary fibrosis 1 year after a single PHMG-p exposure [13]. Therefore, it is important to observe the impacts of combined exposure to PM underlying PHMG-p-induced lung injury.

Previously, several studies have demonstrated the occurrence of increased lung fibrosis or inflammation after acute or subacute PM exposure with or without underlying bleomycin-induced fibrosis in rodents [20–24]. Notably, it is well known that lung fibrosis due to bleomycin resembles idiopathic pulmonary fibrosis in human [25,26]. Also, combined exposure to formaldehyde and $PM_{2.5}$ has been shown to have a synergistic effect, causing more severe damage in asthmatic mice [27]. As shown in these research results, in the presence of underlying lung disease, PM has a greater impact, and it can cause more severe lung damage.

In the present study, we used chest CT and histopathologic examination to show that PM exacerbates PHMG-induced pulmonary fibrosis and inflammation. PM has been shown to upregulate inflammatory cytokines and trigger oxidative stress, causing pulmonary damage even after only a single exposure in a mouse model [28–30]. In humans, it is well known that PM impairs lung function, primarily in susceptible populations, such as older adults or people with chronic obstructive pulmonary disease [31–33]. Therefore, individuals with PHMG-p–induced lung injury who are exposed to PM are likely to suffer from more severe lung inflammation and increased fibrosis. Additionally, reducing and avoiding PM exposure in patients who have underlying lung disease is important for safeguarding public health and mitigating the adverse effects of air pollution. Comprehensive regulatory measures, combined with public education and awareness efforts, are essential steps toward achieving this goal.

We performed quantitative CT analysis to detect lung lesions, including those reflecting lung fibrosis and inflammation. To date, there have been several thresholds of Hounsfield unit (HU) ranges used to define normal and pathologic lung tissue in animal models. For example, Bell et al. used a threshold of −256 HU to determine the presence of interstitial lung disease due to rheumatoid arthritis in a mouse model [34]. Perez et al. used between −200 HU and 200 HU for defining radiation-induced injury in a rat model [35]. Reske et al. defined normal lung tissue as between −900 and −500 HU in pig and sheep models [36]. In our study, we used HU values between −200 and −600 HU to define lesions in lungs, including fibrosis and inflammation, respectively, according to previous studies [37–39]. However, there were some cases that did not involve all significant lesions, including lung fibrosis and inflammation induced by PHMG-p and PM when using these criteria. Hence, in our study, lesions falling outside this range (between −200 and −600 HU) were also classified as lung lesions if deemed by the reviewing radiologist to indicate lung fibrosis or inflammation. Setting standardized density thresholds for characterizing lung disease might be important in quantitative CT analyses; however, as the density can change depending on CT scan parameters, breathing conditions, and animal types, the definitions inevitably depend more on the decisions of experts. Indeed, when interpreting chest CT scans of human patients, it is often more practical to assess the presence or absence of lesions based on the radiologist's judgment rather than adhering strictly to predefined threshold criteria.

Our study did not find statistically significant differences between the PM group and the control group in terms of the number of lung tumors, although there was a higher mean tumor count observed in the PM group. All rats exhibited bronchiolo-alveolar hyperplasia, and only two rats in the PM group exhibited bronchiolo-alveolar adenomas. In a previous 1-year PHMG-p exposure study, following PHMG-p exposure, there was a significant increase in the number of bronchiolo-alveolar hyperplasia lesions over time, with carcinomas detected 52 weeks after PHMG-p instillation [13]. In our study, we sacrificed all rats at 12 weeks after PHMG-p instillation, and the mean numbers of bronchiolo-alveolar hyperplasia lesions in the PM group and the control group were 10.70 ± 6.55 and 8.70 ± 7.82, respectively. Therefore, none of the tumors that developed in our study were PM-associated lung tumors, and the carcinogenic effect of PM could be considered weak. Nevertheless, several studies have explored the link between particulate matter (PM) and lung cancer, as well as the genetic mechanisms that contribute to the carcinogenic effects of PM [40]. Therefore, further studies with long-term follow-up should be conducted to draw firmer conclusions about the carcinogenic effects of PM.

There were several limitations to this study. First, the saline buffer containing the extracted PM was filtered through a 0.2-μm syringe filter to eliminate any quartz particles present in the PM suspension. This filtration step was implemented to mitigate the potential impact of quartz components on the lungs, but it is recognized that the utilization of a saline buffer may have led to the removal of specific non-water soluble constituents from PM or some other important PM components. Therefore, we analyzed the PM components and have listed them in Supplementary Table 2. We considered that the impact of PM demonstrated in this study was only due to the components listed in Supplementary Table 2. Second, molecular experiments were not performed. Since the main objective was to demonstrate the effects of subchronic PM exposure underlying lung fibrosis due to PHMG-p exposure using chest CT and histopathologic analyses, lung tissue was not available for molecular experiments. However, future research should prioritize molecular investigations to assess and validate the influence of PM on PHMG-p–induced lung injury. Third, we did not evaluate the chronic effects of PM exposure on PHMG-p–induced lung injury. In a real-world context, chronic PM exposure might be more common than subchronic PM exposure; therefore, it will be important to explore longer-term effects in future studies.

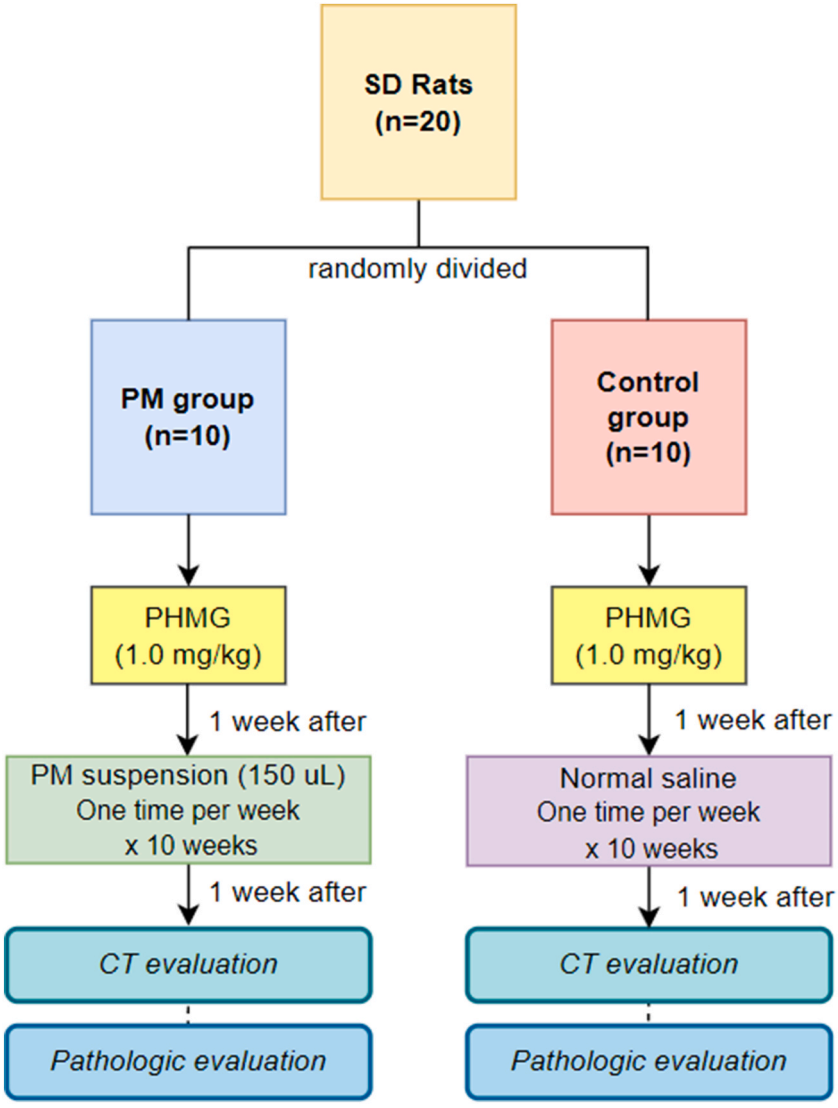

Fig. 3. Summary of the experimental design.

In conclusion, subchronic exposure to PM exacerbated pulmonary inflammation and fibrosis in the context of PHMG-p–induced lung injury. These outcomes were substantiated through comprehensive quantitative and qualitative analyses of chest CT scans, along with histopathologic examination.

4. Materials and methods

This study received approval from the Institutional Animal Care and Use Committee of Korea University Medical Center (approval number: Korea-2023-0054).

4.1. Animals

Eight-week-old male Sprague-Dawley rats (Raonbio, Yong-in, South Korea) underwent a one-week acclimatization period. Environmental conditions were strictly controlled: temperatures were maintained between 22 and 25 °C, relative humidity was kept between 40 and 60 %, and the rats were exposed to a 12-h light/dark cycle. They had unrestricted access to pelleted food (Purina, Sung-nam, South Korea) and filtered tap water throughout the study period. Across the study's timeline, assorted facets were subjected to consistent scrutiny. These encompassed the systematic monitoring of the rats' weekly weight fluctuations, meticulous observations of their physiological states (entailing the identification of indicators like coarse fur, anomalous postures, or dilated pupils), quantitative evaluation of clinical benchmarks (encompassing a $\geq$50 % escalation in cardiac and respiratory rhythms, or conspicuously

diminished rates), attentive surveillance of spontaneous behavioral patterns (comprising the identification of unanticipated vocalizations, instances of self-inflicted harm, restlessness, or extended periods of immobility), and precise measurement of their responses to external stimuli (entailing documentation of aggressive reactions or states of unconsciousness). The responsibility for carrying out these evaluations lay in the hands of adept personnel affiliated with the specialized facility. Instances where the rats exhibited marked frailty, incurred a 20 % loss in initial body weight preceding the study, or evinced compromised mobility, feeding, or drinking due to the presence of tumors, warranted contemplation of euthanasia. It is imperative to underscore, however, that throughout the study's duration, no rats were subjected to euthanasia on the grounds of these conditions.

4.2. Filtered liquid fine PM collection

With the use of a high-capacity air sampling device (HV-1700RW, Sibata, Tokyo, Japan) with quartz filtration (QR-100, Sibata), atmospheric particulate matter (PM) was systematically collected on a weekly basis, 5 days each week, atop the Korea University Ansan Hospital in Gyeonggi province, South Korea. The air sampler operated at a flow rate of 1000 L/min for 23 h a day. To prepare for PM extraction, PM filters were first desiccated using an automated desiccator (Sanpla Dry Keeper, Sanplatec Co., Osaka, Japan). Given that air sampling required one filter per day, a total of seven filters were meticulously chosen in accordance with the World Health Organization's directives for $PM_{2.5}$ (mean exceeding 25 $\mu g/m^3$ per day) and PM_{10} (mean exceeding 50 $\mu g/m^3$ per day) real-time air quality monitoring standards (https://www.airkorea.or.kr/eng). The specific dates chosen for the air sampling were November 26, 2018; January 15, 2019; January 22, 2019; March 26, 2019; March 27, 2019; April 22, 2019; and May 23, 2019 (Supplementary Table 1).

For the formulation of the PM suspension, the quartz filters housing the PM were sectioned into smaller segments (2 × 2 cm) and submerged in 160 mL of a 0.9 % saline buffer solution. After 30 min of sonication and an additional 10 min of agitation, the saline buffer was subjected to filtration via a 0.2-μm syringe filter. This filtration step aimed to eliminate any quartz residue that could potentially mingle with the PM suspension. Detailed composition information of the final PM suspension can be found in Supplementary Table 2.

4.3. Experimental design

Fig. 3 presents a schematic representation of the experimental setup. A cohort of 20 rats was subjected to random assignment and divided into the PM group (consisting of 10 rats subjected to PHMG-p + PM treatment) and the control group (comprising 10 rats subjected to PHMG-p + normal saline treatment). Given that the collected PM samples were adhered to filters, in order to extract the PM and perform intratracheal instillation, the samples had to be submerged using normal saline. Since normal saline was used in the PM suspension, normal saline was administered to the control group in our experiment to achieve the same conditions as the PM group.

For anesthesia induction, all rats were exposed to 2 % isoflurane in a blend of 70 % N_2O and 30 % O_2. This was followed by the intratracheal administration of a PHMG solution (1.0 mg/kg). After an initial week of PHMG exposure, recurring intratracheal installations of PM suspension (150 μL) or normal saline commenced. This regimen continued for 10 weeks, with interventions facilitated through modified videoscopic guidance. The total accumulation over the 10-week period equated to 1.5 mL (one instillation [150 μL] per week × 10 times = total 1.5 mL over 10 weeks).

The volume of air inhaled by an average individual (weighing 60 kg) is approximately 9660 L/day (https://www.epa.gov/expobox/exposure-assessment-tools-routes), while the air sampler's suction capacity was measured at 1,380,000 L/day. Therefore, the volume of air sampled by the device across 7 days simulated the inhalation volume of a human across 1000 days (1,380,000 L/day × 7 days/9660 L/day = 1000 days). In this particular investigation, the contents of seven filters, collected over a 7-day interval, were extracted into a saline buffer amounting to 160 mL. Given that this volume (160 mL) equated to the extent of human exposure over 1000 days, it was deduced that daily human exposure is about 0.160 mL of PM suspension (160 mL/1000 days = 0.160 mL/day). Therefore, a human's daily exposure was approximated at 0.16 mL. Meanwhile, the cumulative dosage administered to the rats reached 1.5 mL. It was inferred that the aggregate amount administered to the rats (1.5 mL) was equivalent to the extent of human PM exposure over 9.38 days or 225.1 h (1.5 mL/0.16 mL/day = 9.38 days; 9.38 days × 24 h/day = 225.1 h).

4.4. CT protocol

One week following the final intratracheal instillation of either PM suspension or normal saline, all rats underwent CT scans. Imaging was conducted using a Philips IQon 128-slice dual-layer detector spectral CT scanner (Philips Healthcare, Cleveland, OH, USA) with the rats positioned supine. CT images were systematically acquired from the lung base to the thoracic inlet in a caudocranial direction, with animals holding their breath in inspiration facilitated by a small-animal ventilator (VentElite, Harvard Apparatus, MA, USA). Each scan lasted less than 10 s per rat. The CT scan parameters were as follows: 80 kVp, 400 mA; collimation, 64 × 0.625 mm; slice thickness, 0.67 mm; beam width, 40 mm; pitch, 1.048; and rotation time, 0.4 s.

4.5. Qualitative CT analysis

All CT images were qualitatively analyzed by a board-certified radiologist specializing in thoracic imaging (C.K.), who had 12 years of experience in the field. The radiologist was blinded to the group allocations during the analysis. The evaluation included features such as consolidation, ground-glass opacity (GGO), centrilobular nodules, nodules, masses, bronchiectasis, and linear densities. These

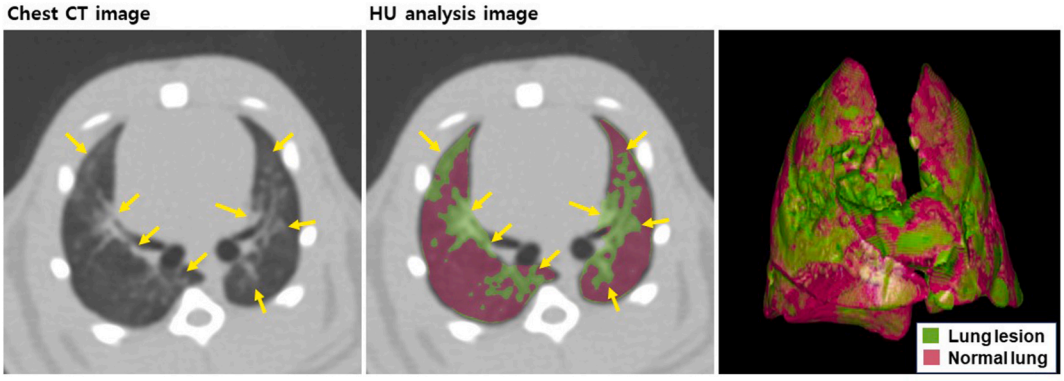

Category	Lesion volume (mL)	Lesion Volume percentage (out of whole lung)
Lung lesion	3.72	26.9
Whole lung	13.83	100

Fig. 4. An example of the quantitative CT evaluation of a rat in the PM group. Green represents lung lesions, and pink represents the normal lung tissue. The lung lesion volume (mL) of this rat was 3.72 mL, and the lesion volume percentage was 26.9 %.

features were assessed and modified according to the Fleischner Society's glossary of radiologic terms for human chest CT [14] and previous studies (Supplementary Table 3). Among the CT findings, consolidation and GGO were considered inflammation, and bronchiectasis and linear densities were considered fibrosis. These CT findings were assessed in the four right lung lobes and the three regions of the left lung according to previous studies [8,12,13,15]. The extent of CT findings was scored as follows: 0 = none, 1 = lesions involving 1–25 % of a lobe, 2 = lesions involving 26–50 % of a lobe, 3 = lesions involving 51–75 % of a lobe, and 4 = lesions involving 76–100 % of a lobe. This was termed the "CT extent score." The "total CT score" was the sum of the scores for any CT findings in both lungs. The "CT inflammation score" was defined as the sum of the CT scores for consolidation and GGO, while the "CT fibrosis score" was the sum of the CT scores for bronchiectasis and linear densities.

4.6. Quantitative CT analysis

All CT images underwent quantitative analysis of the pixel HU (Hounsfield Unit) distributions using a software (IntelliSpace Portal, Philips). Based on previous studies, fibrotic lung lesions typically have HU values between −200 and −600 HU. Thus, in rat lung CT images, any area with HU values within this range was considered a lung lesion. Additionally, lesions falling outside this range were identified if the reviewing radiologist determined them to represent lung abnormalities, such as signs of inflammation and fibrosis. The study quantified lesion volume (the volume of lung lesions), whole-lung volume, and lesion volume percentage (volume of lung lesions/whole-lung volume × 100). All evaluations, including CT image readings and analyses, were performed by a board-certified radiologist specializing in thoracic imaging (C.K.), who remained blinded to the group allocations throughout. Fig. 4 illustrates an example of the quantitative CT evaluation.

4.7. Histologic examination

All lung specimens were evaluated by a pathologist specializing in thoracic pathology (J.L.), who has 22 years of expertise in the field. The lungs were fixed in 10 % neutral buffered formalin. Thin sections of 4 μm were prepared from these samples and then stained with hematoxylin and eosin (H&E) as well as Masson's trichrome stain.

We evaluated the inflammation using the following criteria: extent (none, involving <25 %, 25 %–50 %, >50 % of total lung area) and severity (none, mild, moderate, severe). Pathologic inflammation scores were derived by combining extent and severity scores, where extent scores were categorized as 0 = none, 1 = <25 %, 2 = 25 %–50 %, and 3 = >50 % of the entire lung, and severity scores as 0 = none, 1 = mild, 2 = moderate, and 3 = severe. For quantifying fibrosis, we utilized the Modified Ashcroft scoring method [41]. Additionally, we assessed the numbers of bronchiolo-alveolar hyperplasia and bronchiolo-alveolar adenomas across all experimental groups.

4.8. Statistical analysis

Statistical comparisons between CT features and histopathologic findings were conducted using the chi-square test for nominal variables and the Mann-Whitney *U* test for continuous variables (IBM SPSS Statistics for Windows, version 20, IBM Corp., Armonk, NY, USA). A significance level of $P < 0.05$ was applied to determine statistical significance.

Data availability statement

The data will be available with reasonable request after contacting the corresponding authors.

CRediT authorship contribution statement

Cherry Kim: Writing – review & editing, Writing – original draft, Visualization, Validation, Software, Resources, Project administration, Methodology, Investigation, Formal analysis, Data curation, Conceptualization. **Sang Hoon Jeong:** Writing – original draft, Visualization, Validation, Resources, Project administration, Methodology, Formal analysis, Data curation, Conceptualization. **Hong Lee:** Investigation, Formal analysis, Data curation, Conceptualization. **Yoon Jeong Nam:** Project administration, Methodology, Investigation. **Hyejin Lee:** Methodology, Investigation. **Jin Young Choi:** Methodology, Investigation. **Yu-Seon Lee:** Methodology, Investigation. **Jaeyoung Kim:** Methodology, Investigation. **Yoon Hee Park:** Software, Methodology, Investigation. **Ju-Han Lee:** Writing – review & editing, Writing – original draft, Visualization, Validation, Supervision, Resources, Project administration, Methodology, Investigation, Funding acquisition, Formal analysis, Data curation, Conceptualization.

Declaration of competing interest

The authors declare that they have no known competing financial interests or personal relationships that could have appeared to influence the work reported in this paper.

Acknowledgments

This work was supported by the National Research Foundation of Korea (NRF) grant funded by the Korea government (MSIT) (RS-2024-00342750), along with grants from Korea University Ansan Hospital and Korea University. This research also received funding from the Korea Ministry of Environment under the Environmental Health Action Program (2018001360002). We extend our gratitude to Meehye Lee and Joo-Ae Kim for their contributions to analyzing the concentrations of inorganic ions and water-soluble organic carbon in the PM samples utilized in this investigation.

Appendix A. Supplementary data

Supplementary data to this article can be found online at https://doi.org/10.1016/j.heliyon.2024.e34562.

References

[1] A.J. Cohen, et al., Estimates and 25-year trends of the global burden of disease attributable to ambient air pollution: an analysis of data from the Global Burden of Diseases Study 2015, Lancet 389 (2017) 1907–1918, https://doi.org/10.1016/S0140-6736(1730505-6.
[2] A.J. Cohen, et al., Estimates and 25-year trends of the global burden of disease attributable to ambient air pollution: an analysis of data from the Global Burden of Diseases Study 2015, Lancet 389 (2017) 1907–1918.
[3] W. Hill, et al., Lung adenocarcinoma promotion by air pollutants, Nature 616 (2023) 159–167, https://doi.org/10.1038/s41586-023-05874-3.
[4] R. Xu, et al., Acute effects of exposure to fine particulate matter and ozone on lung function, inflammation and oxidative stress in healthy adults, Ecotoxicol. Environ. Saf. 243 (2022) 114013, https://doi.org/10.1016/j.ecoenv.2022.114013.
[5] C.H. Chen, et al., The effects of fine and coarse particulate matter on lung function among the elderly, Sci. Rep. 9 (2019) 14790, https://doi.org/10.1038/s41598-019-51307-5.
[6] Q. Hu, et al., Linkage between particulate matter properties and lung function in schoolchildren: a panel study in southern China, Environ. Sci. Technol. 54 (2020) 9464–9473, https://doi.org/10.1021/acs.est.9b07463.
[7] G.C. Goobie, et al., Association of particulate matter exposure with lung function and mortality among patients with fibrotic interstitial lung disease, JAMA Intern. Med. 182 (2022) 1248–1259, https://doi.org/10.1001/jamainternmed.2022.4696.
[8] C. Kim, et al., Evaluation of the effect of filtered ultrafine particulate matter on bleomycin-induced lung fibrosis in a rat model using computed tomography, histopathologic analysis, and RNA sequencing, Sci. Rep. 11 (2021) 22672, https://doi.org/10.1038/s41598-021-02140-2.
[9] H.R. Kim, G.W. Hwang, A. Naganuma, K.H. Chung, Adverse health effects of humidifier disinfectants in Korea: lung toxicity of polyhexamethylene guanidine phosphate, J. Toxicol. Sci. 41 (2016) 711–717, https://doi.org/10.2131/jts.41.711.
[10] J.A. Song, et al., Polyhexamethyleneguanidine phosphate induces severe lung inflammation, fibrosis, and thymic atrophy, Food Chem. Toxicol. : an international journal published for the British Industrial Biological Research Association 69 (2014) 267–275, https://doi.org/10.1016/j.fct.2014.04.027.
[11] S. Kim, D. Paek, Humidifier disinfectant disaster: what is known and what needs to be clarified, Environ Health Toxicol 31 (2016) e2016025, https://doi.org/10.5620/eht.e2016025.
[12] S.H. Jeong, et al., Longitudinal long term follow up investigation on the carcinogenic impact of polyhexamethylene guanidine phosphate in rat models, Sci. Rep. 14 (2024) 7178, https://doi.org/10.1038/s41598-024-57605-x.
[13] C. Kim, et al., Evaluation of the long-term effect of polyhexamethylene guanidine phosphate in a rat lung model using conventional chest computed tomography with histopathologic analysis, PLoS One 16 (2021) e0256756, https://doi.org/10.1371/journal.pone.0256756.
[14] D.M. Hansell, et al., Fleischner Society: glossary of terms for thoracic imaging, Radiology 246 (2008) 697–722, https://doi.org/10.1148/radiol.2462070712.
[15] C. Kim, et al., Evaluation of polyhexamethylene guanidine-induced lung injuries by chest CT, pathologic examination, and RNA sequencing in a rat model, Sci. Rep. 11 (2021) 6318, https://doi.org/10.1038/s41598-021-85662-z.
[16] Y.G. Lee, P.H. Lee, S.M. Choi, M.H. An, A.S. Jang, Effects of air pollutants on airway diseases, Int. J. Environ. Res. Publ. Health 18 (2021), https://doi.org/10.3390/ijerph18189905.
[17] T. Li, Y. Yu, Z. Sun, J. Duan, A comprehensive understanding of ambient particulate matter and its components on the adverse health effects based from epidemiological and laboratory evidence, Part. Fibre Toxicol. 19 (2022) 67, https://doi.org/10.1186/s12989-022-00507-5.

[18] J. Song, W. Kim, Y.B. Kim, B. Kim, K. Lee, Time course of polyhexamethyleneguanidine phosphate-induced lung inflammation and fibrosis in mice, Toxicol. Appl. Pharmacol. 345 (2018) 94–102, https://doi.org/10.1016/j.taap.2018.02.013.
[19] M.K. Song, D.I. Kim, K. Lee, Time-course transcriptomic alterations reflect the pathophysiology of polyhexamethylene guanidine phosphate-induced lung injury in rats, Inhal. Toxicol. 31 (2019) 457–467, https://doi.org/10.1080/08958378.2019.1707912.
[20] B. Sun, et al., Short-term PM2. 5 exposure induces sustained pulmonary fibrosis development during post-exposure period in rats 385 (2020) 121566.
[21] Z. Xu, et al., PM(2.5) induced pulmonary fibrosis in vivo and in vitro, Ecotoxicol. Environ. Saf. 171 (2019) 112–121, https://doi.org/10.1016/j.ecoenv.2018.12.061.
[22] Y. Shi, et al., PM2.5-induced alteration of DNA methylation and RNA-transcription are associated with inflammatory response and lung injury, Sci. Total Environ. 650 (2019) 908–921, https://doi.org/10.1016/j.scitotenv.2018.09.085.
[23] M. Marinova, P. Solopov, C. Dimitropoulou, R.M.L. Colunga Biancatelli, J.D. Catravas, Acute exposure of mice to hydrochloric acid leads to the development of chronic lung injury and pulmonary fibrosis, Inhal. Toxicol. 31 (2019) 147–160, https://doi.org/10.1080/08958378.2019.1624895.
[24] I.Y. Cheng, et al., Particulate matter increases the severity of bleomycin-induced pulmonary fibrosis through KC-mediated neutrophil chemotaxis, Int. J. Mol. Sci. 21 (2019), https://doi.org/10.3390/ijms21010227.
[25] D.N. O'Dwyer, B.B. Moore, Animal models of pulmonary fibrosis, Methods Mol. Biol. 1809 (2018) 363–378, https://doi.org/10.1007/978-1-4939-8570-8_24.
[26] J.D. Williamson, L.R. Sadofsky, S.P. Hart, The pathogenesis of bleomycin-induced lung injury in animals and its applicability to human idiopathic pulmonary fibrosis, Exp. Lung Res. 41 (2015) 57–73, https://doi.org/10.3109/01902148.2014.979516.
[27] X. Lu, et al., Impacts of combined exposure to formaldehyde and PM(2.5) at ambient concentrations on airway inflammation in mice, Environ. Pollut. 315 (2022) 120234, https://doi.org/10.1016/j.envpol.2022.120234.
[28] L. Risom, P. Møller, S. Loft, Oxidative stress-induced DNA damage by particulate air pollution, Mutat. Res. 592 (2005) 119–137, https://doi.org/10.1016/j.mrfmmm.2005.06.012.
[29] K.E. Driscoll, R.C. Lindenschmidt, J.K. Maurer, J.M. Higgins, G. Ridder, Pulmonary response to silica or titanium dioxide: inflammatory cells, alveolar macrophage-derived cytokines, and histopathology, Am. J. Respir. Cell Mol. Biol. 2 (1990) 381–390, https://doi.org/10.1165/ajrcmb/2.4.381.
[30] J.L. Quay, W. Reed, J. Samet, R.B. Devlin, Air pollution particles induce IL-6 gene expression in human airway epithelial cells via NF-kappaB activation, Am. J. Respir. Cell Mol. Biol. 19 (1998) 98–106, https://doi.org/10.1165/ajrcmb.19.1.3132.
[31] J. McCreanor, et al., Respiratory effects of exposure to diesel traffic in persons with asthma, N. Engl. J. Med. 357 (2007) 2348–2358, https://doi.org/10.1056/NEJMoa071535.
[32] J.T. Lee, J.Y. Son, Y.S. Cho, The adverse effects of fine particle air pollution on respiratory function in the elderly, Sci. Total Environ. 385 (2007) 28–36, https://doi.org/10.1016/j.scitotenv.2007.07.005.
[33] S. Lagorio, et al., Air pollution and lung function among susceptible adult subjects: a panel study, Environ. Health 5 (2006) 11, https://doi.org/10.1186/1476-069x-5-11.
[34] R.D. Bell, C. Rudmann, R.W. Wood, E.M. Schwarz, H. Rahimi, Longitudinal micro-CT as an outcome measure of interstitial lung disease in TNF-transgenic mice, PLoS One 13 (2018) e0190678, https://doi.org/10.1371/journal.pone.0190678.
[35] J.R. Perez, et al., A comparative analysis of longitudinal computed tomography and histopathology for evaluating the potential of mesenchymal stem cells in mitigating radiation-induced pulmonary fibrosis, Sci. Rep. 7 (2017) 9056, https://doi.org/10.1038/s41598-017-09021-7.
[36] A.W. Reske, et al., Extrapolation in the analysis of lung aeration by computed tomography: a validation study, Crit. Care 15 (2011) R279, https://doi.org/10.1186/cc10563.
[37] B. Sul, et al., Volumetric characteristics of idiopathic pulmonary fibrosis lungs: computational analyses of high-resolution computed tomography images of lung lobes, Respir. Res. 20 (2019) 216, https://doi.org/10.1186/s12931-019-1189-5.
[38] S.Y. Ash, et al., Densitometric and local histogram based analysis of computed tomography images in patients with idiopathic pulmonary fibrosis, Respir. Res. 18 (2017) 45, https://doi.org/10.1186/s12931-017-0527-8.
[39] D.J. Lederer, et al., Cigarette smoking is associated with subclinical parenchymal lung disease: the Multi-Ethnic Study of Atherosclerosis (MESA)-lung study, Am. J. Respir. Crit. Care Med. 180 (2009) 407–414, https://doi.org/10.1164/rccm.200812-1966OC.
[40] H. Liu, X. Zhang, Z. Sun, Y. Chen, Ambient fine particulate matter and cancer: current evidence and future perspectives, Chem. Res. Toxicol. 36 (2023) 141–156, https://doi.org/10.1021/acs.chemrestox.2c00216.
[41] R.H. Hubner, et al., Standardized quantification of pulmonary fibrosis in histological samples, Biotechniques 44 (507–511) (2008), https://doi.org/10.2144/000112729, 514-507.